Effects of optogenetic stimulation of vasopressinergic retinal afferents on suprachiasmatic neurons

Catherine Hume[1], Andrew Allchorne[1], Valery Grinevich[3], Gareth Leng[1] and Mike Ludwig[1,2]

[1]Centre for Discovery Brain Sciences, University of Edinburgh, Edinburgh, UK
[2]Centre for Neuroendocrinology, University of Pretoria, Pretoria, South Africa
[3]Department of Neuropeptide Research, Central Institute of Mental Health, University Heidelberg, Mannheim, Germany.

Correspondence to:
Mike Ludwig
Centre for Discovery Brain Sciences, University of Edinburgh, Hugh Robson Building, George Square, Edinburgh EH8 9XD, UK
Tel: -44 (0) 131 650 3275
email: mike.ludwig@ed.ac.uk

Keywords: vasopressin, SCN, channelrhodopsin, optogenetics, retina

Abstract

Physiological circadian rhythms are orchestrated by the hypothalamic suprachiasmatic nucleus (SCN). The activity of SCN cells is synchronised by environmental signals, including light information from retinal ganglion cells (RGCs). We recently described a population of vasopressin-expressing RGCs (VP-RGC) which send axonal projections to the SCN. To determine how these VP-RGCs influence the activity of cells in the SCN, we used optogenetic tools to specifically activate their axon terminals within the SCN. Rats were intravitreally injected with a recombinant adeno-associated virus (rAAV) to express the channelrhodopsin-2 and the red fluorescent protein mCherry under the vasopressin promoter (VP-ChR2mCherry). *In vitro* recordings in acute brain slices showed that approximately 30% of ventromedial SCN cells responded to optogenetic stimulation with an increase in firing rate that progressively increased during the first 200 s of stimulation and which persisted after the end of stimulation. Finally, application of a vasopressin V1A receptor antagonist dampened the response to optogenetic stimulation. Our data suggest that optogenetic stimulation of VP-RGC axons within the SCN influences the activity of SCN cells in a vasopressin dependent manner.

Introduction

In all animals, the transition between night and day engages a host of physiological and behavioural rhythms. A subset of retinal ganglion cells (RGCs) that express melanopsin detect the ambient light level, and they project to the suprachiasmatic nucleus (SCN) of the hypothalamus to entrain circadian rhythms that are generated within the SCN (1-4). We have recently shown that a subpopulation of these RGCs express the neuropeptide vasopressin (VP-RGCs). The electrical activity of VP-RGCs is stimulated by light, and vasopressin concentrations in the SCN, measured by microdialysis *in vivo*, increase following light exposure (5).

Vasopressin is also expressed in many neurons of the dorsolateral SCN shell, and these have a critical role in maintaining circadian rhythms (6). SCN vasopressin concentrations and the expression of vasopressin V1A receptors in the SCN are under circadian control (7, 8) and transgenic mice deficient in vasopressin V1A receptors show dampened circadian rhythms in the absence of light-cues (8). Additionally, infusion of vasopressin V1 antagonists into the SCN speeds up re-entrainment of mice to a new light dark cycle when the light phase is shifted experimentally (9).

The vasopressin cells in the SCN shell are not direct recipients of signals from the VP-RGCs; the projections from the retina innervate just the ventromedial 'core' of the SCN, which contains neurones expressing other neuropeptides, including vasoactive intestinal peptide (VIP) and gastrin-releasing peptide (GRP) (10). Light exposure and stimulation of the retino-hypothalamic tract increases the electrical activity of ventromedial SCN core neurons *in vivo,* and these responses are attenuated by the local application of a vasopressin V1A receptor antagonist (5). Together these studies suggest that activation of VP-RGCs results in vasopressin release in the SCN, which in turn influences the electrical activity of SCN core neurons.

However, the source from which vasopressin is secreted into the SCN following light exposure is unclear. Vasopressin could either be secreted from VP-RGC axon terminals in the SCN core or from the dendrites of vasopressin neurons in the SCN shell. Here, we used optogenetics to selectively activate VP-RGC axons in the SCN, measured the influence of this on the electrical activity of SCN core neurons, and investigated the effects of a V1a receptor antagonist on evoked responses.

Methods

Animals

All experimental procedures were approved by a local ethical committee and carried out under the UK Home Office Animals (Scientific Procedures) Act 1986 by trained personal licence holders. Experiments were performed on a homozygous transgenic rat-line expressing an arginine vasopressin enhanced green fluorescent protein (eGFP) fusion gene (11). Male and female rats of ~7-8 weeks old were used. Rats were housed in same-sex groups in controlled conditions (20-22°C) in a normal 12h dark-light cycle (lights on at 07.00) or shifted dark-light cycle (lights on at 11.00), with *ad lib* access to food and water. Rats were housed in the shifted dark-light cycle for at least two weeks before being used for *in vitro* electrophysiology.

Cloning of rAAV Vectors - Production of rAAVs

rAAV (serotype 1/2) carrying a conserved 1.9kb AVP promoter and cDNA of ChR2 (generously provided by Scott Sternson, Janelia Farm) was cloned and produced as described previously (12, 13). Standard ChR2 was used which has been characterised (14)

and its efficiency confirmed (12, 15, 16). The conserved AVP promoter comprises a 1.9kb sequence has been revealed by BLAT (BLAST-like alignment tool)(16).

Intravitreal virus injection

Rats were anaesthetised with an intraperitoneal injection (IP) of ketamine (75mg/kg) and medetomidine (0.5mg/kg). Once placed in a rotatable stereotaxic frame, a midriatic (phenylephrine 0.0054% and tropicamide 0.00028%), local anaesthetic (oxybuprocaine hydrochloride 0.4%) and antibiotic (ofloxacin 0.3%) were applied to each eye. The head was rotated in the frame and the eye punctured with a fine needle (31G extra short dental cartridge needle, 0.28 x 12mm; Terumo, Belgium) connected to a 5-µl Hamilton syringe and the needle tip lowered into the vitreous humour using a micromanipulator. Two 1-µl injections of virus were carried out on each eye, one on each lateral side. The virus was injected slowly into the eye and the needle left in place for 30s before being slowly retracted. The medetomidine anaesthesia was then reversed with subcutaneous administration of atipamezole (1mg/kg). Rats were left in their home cages for 6-8 weeks before being used for electrophysiology.

In vitro electrophysiology

Experiments were carried out either at the beginning of the light phase (ZT 2) or at the end of the dark phase (ZT 22). From our previous work (5) we anticipated that the amount of vasopressin available for activity-dependent release would be maximal at the end of the dark phase and minimal at the end of the light phase. Accordingly, we studied cells at the end of the dark phase and in the early light phase. Rats subjected to experimental procedures in the dark phase were kept in the dark at all times with no light exposure. Rats were lightly anaesthetised in isoflurane before being decapitated and the brains quickly removed. A small tissue block containing the SCN was cut and immersed in an ice-cold carbogenated N-methyl-D-glucamine (NMDG)-based aCSF cutting solution (92mM NMDG, 2.5mM KCl, 1.25mM NaH_2PO_4, 30mM $NaHCO_3$, 20mM HEPES, 25mM glucose, 2mM thiourea, 5mM Na-ascorbate, 3mM Na-pyruvate, 0.5mM $CaCl_2.4H_2O$ and 10mM $MgSO_4.7H_2O$; pH 7.35) (17) before being sliced into 300-µm sections in partially frozen cutting solution using a vibratome. Brain sections were transferred to a continuously carbogenated NMDG-based aCSF cutting solution in a water bath at 33°C to recover. After 5-10min, brain sections were transferred to a continuously carbogenated HEPES-based aCSF holding solution (92mM NaCl, 2.5mM KCl, 1.25mM NaH_2PO_4, 30mM $NaHCO_3$, 20mM HEPES, 25mM glucose, 2mM thiourea, 5mM Na-ascorbate, 3mM Na-pyruvate, 2mM $CaCl_2.4H_2O$ and 2mM $MgSO_4.7H_2O$) (17) at

room temperature (25°C) for at least 1h before recording. Slices were kept in this same holding solution throughout the day until needed for recording. Slices were transferred to the patch-clamp rig recording chamber and continuously perfused with carbogenated aCSF (119mM NaCl, 2.5mM KCl, 1.25mM NaH_2PO_4, 24mM $NaHCO_3$, 12.5mM glucose, 2mM $CaCl_2.4H_2O$ and 2mM $MgSO_4.7H_2O$) (17) at 25°C. Cells and eGFP fluorescence were viewed using a Zeiss Axioskop 2FS microscope with water immersion objectives and recordings were made using pClamp software (Axon Instruments, Molecular Devices, USA). Individual cells were recorded from in a cell-attached configuration using glass pipettes filled with recording aCSF and a tip resistance of 3-5mΩ. Once the pipette tip was in contact with a cell, a small amount of negative pressure was applied to create a seal with a resistance of 20-80mΩ. Only cells in the ventromedial core region of the SCN were recorded from, and identified based on their location with respect to the optic chiasm and third ventricle (Fig. 1). SCN core neurons receive direct inputs from VP-RGC's (5). Once a stable seal was achieved, at least 100s of baseline activity was recorded. The slices were then optogenetically stimulated for 200 or 500s and continuously recorded from. Optogenetic simulation was achieved by delivering pulses (5ms pulses; 3s on 2s off) of blue light (470nm; 20Hz; optoflash LED light source, Cairn Research Ltd, UK) to the whole slice through the microscope objective. This protocol was selected as the secretion of neuropeptides requires a high-frequency, prolonged stimulation pattern (18). In some experiments, the vasopressin V1A antagonist ($d(CH_2)_5{}^1Tyr(Me)^2Arg^8$)-vasopressin (2μM) (19) was applied to the recording solution once the cells had started to respond to optogenetic stimulation. This antagonist acts at both the vasopressin V1A receptor as well as the oxytocin receptor; however, it is 100 times more selective for the vasopressin V1A receptor than the oxytocin receptor (20). For non-virus transfected controls, SCN cells from VP-eGFP rats were recorded from and the slices exposed to pulses of blue light just as the virus transfected slices were.

Retina Dissection

To create retina flatmounts, eyes were removed following decapitation and the lens and vitreous humour removed by cutting the cornea around the outer edge of the iris. A cut was made down each side of the sclera making sure not to cut the retina then the sclera prised open and the retina removed; 3-4 incisions were made from the perimeter of the retina allowing it to lie flat. On a shaker, the retinas then incubated in heparinised saline for 5min, followed by 0.1M PB for 5min and 4% PFA for 5min. Retinas were then stored in 0.1M PB with 0.02% sodium azide at 4°C until processed for immunohistochemistry.

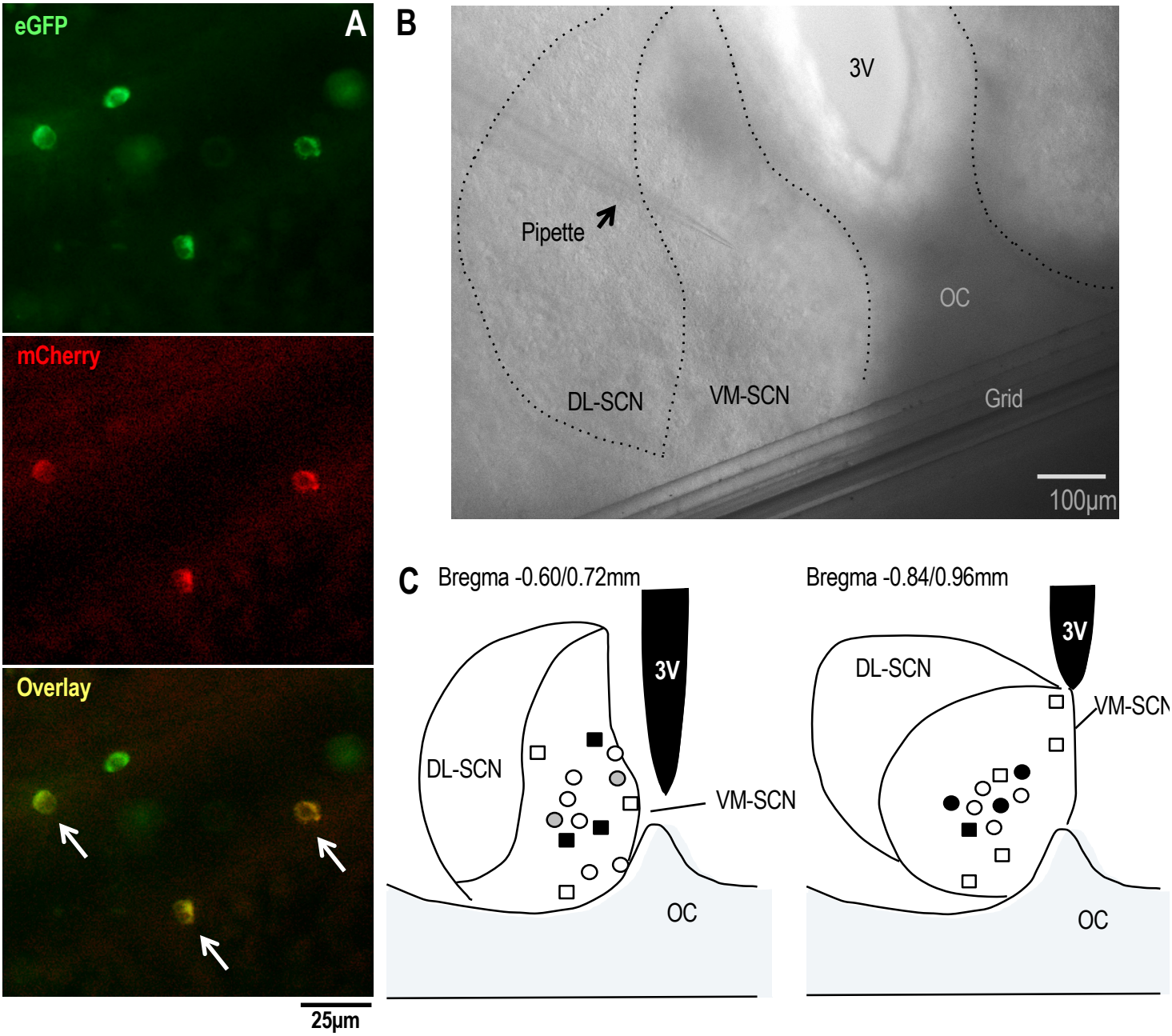

Figure 1) The spatial distribution of ventromedial SCN cells responding to optogenetic stimulation of VP-RGC axons.

A) Viral reporter expression in VP-RGC's in retina flat mounts focused on the retinal ganglion cell layer. Immunohistochemistry for eGFP shown in green, immunohistochemistry for mCherry (viral reporter) shown in red and co-localisation of the two shown in yellow. Arrows point to VP-RGC's expressing mCherry. **B)** The sites of responding ventromedial SCN cells recorded in brain slices. **C)** Diagrams indicating the position of each responding cell recorded mapped onto the rat brain atlas at bregma -0.06/0.72mm and -0.84/0.96mm. White shapes represent cells showing overall increase in firing rate, grey shapes represent cells showing an initial burst of increased firing, and black shapes represent cells whose responses were attenuated by application of a vasopressin V1A receptor antagonist. Circles = recordings from ZT2, squares = ZT22. DL, dorsolateral; OC, optic chiasm; VM, ventromedial; 3V, third ventricle.

Immunohistochemistry

All tissue was processed for free-floating immunohistochemistry as described in (5). Before immunohistochemistry, retinas were incubated in an enzyme mixture containing 0.000072% Collagenase (LS005273; Worthington Chemicals, USA) and 0.001% Hyaluronidase (LS005475; Worthington Chemicals, USA) in the dark for 30min at room temperature with gentle agitation to remove any vitreous humour that may still be attached to the retina (21). After enzyme incubation, retinas were washed in 0.1M PB then incubated in 0.1M glycine in 0.1M PB for 30 min. After washing, retinas were incubated in blocking buffer (10% normal goat serum in 0.1M PB and 0.3% triton-X100) for 1h followed by the primary antibodies against GFP (chicken anti-GFP; 1:1000; Abcam ab13970) and mCherry (rabbit anti-mCherry; 1:100; ThermoFisher Scientific PA5-34974) in blocking buffer (5% normal goat serum in 0.1M PB and 0.3% triton-X100) for 48h at 4°C with gentle agitation. Following washes, the retinas were incubated with goat anti-chicken Alexa Fluor 488 (ThermoFisher Scientific A11039; 1:500) and goat anti-rabbit Alexa Fluor 568 (ThermoFisher Scientific A11011; 1:500) secondary antibodies for 80min diluted in 3% normal goat serum, 0.3% triton-X100 and 0.03% tween in 0.1M PB. The retinas were then mounted onto gelatin-coated slides and coverslips applied with PermaFlour mounting medium. Retina images were taken for analysis using a Leica DMR epifluorescence microscope. Images were processed and co-localization of GFP and mCherry immunofluorescence quantified using Fiji software.

Analysis

All analysis was carried out using ClampFit (Version 10.7, Axon Instruments, Molecular Devices, USA), Microsoft Excel and GraphPad Prism 6 software. The spontaneous firing of SCN cells was recorded for at least 100s before the slice was optogenetically stimulated, and the mean spontaneous firing rate recorded. For each cell firing at > 1 spike/s we constructed an interspike interval (ISI) histogram (in 10-ms bins) of spontaneous activity from the last 100s of baseline recording (22), and calculated the coefficient of variation (CV) as the ratio of the standard deviation/mean ISI. As ISI distributions for slow firing cells were all long-tailed with a conspicuous skew, we also calculated the CV from the log ISIs.

Hazard functions plot how the excitability of a cell evolves with respect to time since the last spike (23). These were constructed from the ISI distribution (in 10-ms bins) according to the formula (hazard in bin [t, t+ 10]) = (number of ISIs in bin [t, t+10])/(number of ISIs of

length > *t*). These functions were truncated at the bin where the residual number of ISIs was < 20.

To assess responses to optogenetic stimulation, for each cell the % change in firing rate was determined from the mean of the last 100s baseline and last 100s during stimulation. Only cells that responded with a mean change in firing rate of ≥10% and a firing rate change of ≥0.5 spikes/s were considered to be responsive.

Statistical Analysis

Data were tested for deviations from normality using a D'Agostino & Pearson omnibus normality test. For data sets that were too small for meaningful normality testing (200s stimulation (n=6), non-parametric statistical tests were used. Larger data sets passed normality testing ($p>0.05$; 500s stimulation (n=12) and VP-GFP cells (n=8)) and parametric statistical tests were used.

Mean baseline firing rates between groups of cells were compared using an unpaired two-tailed t-test. For cells tested with the vasopressin V1A receptor antagonist, the effects of the antagonist on cells activated by optogenetic stimulation were calculated as the difference in firing rate between the last 100 s of optogenetic stimulation and the firing rate in the period 100-200s after antagonist exposure. These changes were compared with the changes measured in cells unresponsive to optogenetic stimulation by an unpaired t-test. Variances of firing rate were compared with an F test (two sample for variances).

Results

VP-RGC viral transfection

Following immunohistochemistry of retina flatmounts, co-localisation of eGFP (vasopressin) and mCherry (viral reporter) was quantified. On average 65.4 ± 8.2% (n=4) of eGFP expressing VP-RGC's co-expressed mCherry for each retina (Fig. 1A). In total, 144 cells out of 243 eGFP+ VP-RGC's co-expressed mCherry, and only one non-eGFP+ cell showed mCherry expression.

Spontaneous activity of ventromedial SCN cells

Recordings were made in SCN slices from 13 rats at the beginning of the light phase (ZT 2) and from 10 rats recorded at the end of the dark phase (ZT 22). Spontaneous firing

rates for ventromedial SCN cells varied from 0.03 to 17.4 spikes/s with a mean (±SEM) firing rate of 4.4 ± 0.4 spikes/s (n=99), similar to rates recorded in previous studies *in vitro* (24). The mean spontaneous firing rate for cells recorded in the light phase (mean 4.5 ± 0.7 spikes/s, range 0.03 to 16.3 spikes/s, n=50) was similar to that of cells recorded in the dark phase (mean 4.4 ± 0.4 spikes/s, range 0.3 to 11.6 spikes/s, n=49). Thus, the spread of firing rates was greater for cells recorded in the light phase than for those in the dark phase ($P<0.001$; F test two sample for variances, $F=3.4$, d.f.48,49).

The regularity of spike activity can be measured by the coefficient of variation of ISIs: a CV value close to 1 is indicative of random firing and a CV value close to 0 is indicative of very regular firing. The mean CV was 0.51± 0.04 (n=49) for cells in the dark phase and significantly larger (0.77 ± 0.06 n=50) for cells in the light phase ($P=0.006$). However, the CV varies with mean firing rate when ISI distributions are long-tailed, so might reflect the greater abundance of slow firing cells in the light phase. If the CV is calculated from the log ISIs it is independent of mean firing rate (i.e. there is no significant correlation between the mean rate and the CV for log-transformed data); the CV of logISIs was 0.077 ± 0.005 in the dark phase and significantly larger at 0.13 ± 0.01 in the light phase ($P<0.001$) (Fig. 2A).

To assess firing patterns, ISI histograms were constructed for all cells with a firing rate above 1.3 spikes/s. Cells recorded in both the light and dark phases showed a unimodal ISI distribution with modes between 60 and 220 ms, depending on mean firing rate. From the ISI histograms and CV values it was apparent that cells recorded in the light phase were individually more irregular in their spiking (as reflected in the significant difference between the CV of logISIs as shown in Fig. 2A). These cells also had a wider range of mean spontaneous firing rates (Fig. 2A).

Hazard functions were constructed from ISI histograms to assess activity-dependent influences on excitability in each cell. Cells firing at less than 1.3 spikes/s were excluded from hazard function analysis (16 light phase cells and 5 dark phase cells). The individual hazard functions shapes for the other 78 ‘active’ cells (firing rate >1.3 spikes/s) were strongly dependent on firing rate i.e. speed of inferred repolarisation following a spike (Fig. 2B). We split these cells into three groups of 26 on the basis of firing rate and plotted the mean hazard function for these groups (Fig. 2B). The fastest firing rate group (mean 8.5 ± 0.8 spikes/s; range 6.3-16.3), distinguished by the steepest hazard function plot, contained 16 cells in the light phase (Fig. 2C-E) and 10 cells in the dark phase; the middle firing rate group (mean 4.5 ± 0.2 spikes/s; range 3.3-6.3) contained 7 in the light phase and 17 in the dark phase; and the slow firing rate group (mean 2.3 ± 0.1 spikes/s; range 1.3-3.2)

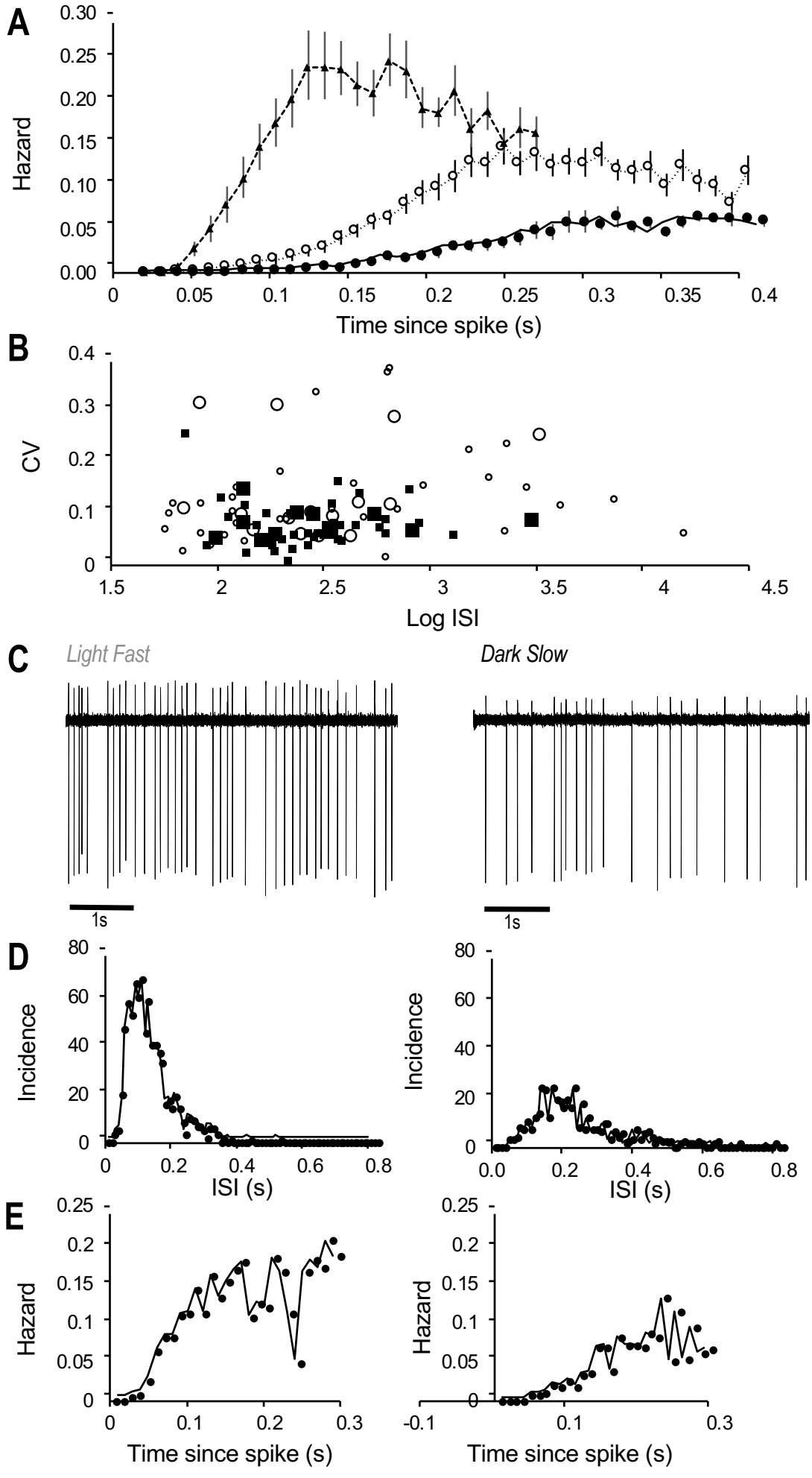
A
Hazard
0.30
0.25
0.20
0.15
0.10
0.05
0.00
0
0.05
0.1
0.15
0.2
0.25
0.3
0.35
0.4
Time since spike (s)
B
CV
0.4
0.3
0.2
0.1
0
1.5
2
2.5
3
3.5
4
4.5
Log ISI
C
Light Fast
Dark Slow
1s
1s
D
Incidence
80
60
40
20
0
0
0.2
0.4
0.6
0.8
ISI (s)
Incidence
80
60
40
20
0
0.0
0.2
0.4
0.6
0.8
ISI (s)
E
Hazard
0.25
0.2
0.15
0.1
0.05
0
0
0.1
0.2
0.3
Time since spike (s)
Hazard
0.25
0.2
0.15
0.1
0.05
0
-0.1
0.1
0.3
Time since spike (s)

Figure 2. Spontaneous activity of SCN cells

A) Mean (±S.E.) hazard functions of SCN light and dark phase neurons in 10-ms bins constructed from 100 s of spontaneous activity. Hazard functions were constructed only for the 78 cells firing at >1.3 spike/s. The cells were separated into three groups of 26 cells by their mean firing rate. The fast firing cells (triangles) fired at a mean rate of 8.5 ± 0.8 spikes/s, the middle group (open circles) at 4.5 ± 0.2 spikes/s and the slow cells (closed circles) at 2.3 ± 0.1 spikes/s. **B)** CV of log ISI plotted against mean log ISI for all spontaneously active SCN cells firing at >1.3 spikes/s. Open symbols: cells recorded in the light phase; closed symbols: cells recorded in the dark phase. The large symbols are cells activated by optogenetic stimulation, the small symbols are cells unresponsive to stimulation. **C)** Extracts of the raw spike traces for a representative light-phase cell with a fast repolarization (left panel) and dark-phase cell with a slow repolarization (right panel). **D)** ISI histograms for the two cells shown in B and **E)** corresponding hazard functions.

contained 10 cells in the light phase and 16 in the dark phase (Fig. 2C-E). These hazard functions demonstrate that cells recorded in both light and dark phases display a similar range of repolarization speeds.

Responses of ventromedial SCN cells to optogenetic stimulation

Fifteen of 50 ventromedial SCN cells recorded in the light phase and 12 of 49 cells recorded in the dark phase responded to optogenetic stimulation with a change in firing rate of >10% and at least 0.5 spikes/s. As cells in the dark and light phases had similar baseline firing rates and as similar proportions responded to optogenetic stimulation, the responses were analysed together.

Twenty-one SCN cells were tested with 200s of optogenetic stimulation. Six showed increased firing rate throughout stimulation (baseline 6.4 ± 1.1 spikes/s, stimulation 8.8 ± 1.4 spikes/s; (Fig. 3A,D,E). A large, narrow ISI histogram peak and steep hazard function plot can be seen with optogenetic stimulation demonstrating increased firing frequency and faster repolarization (Fig. 3B,C). The mean change in firing rate for these six cells was 2.4 ± 0.8 spikes/s, whereas the mean change in firing rate for the 15 non-responsive cells was -0.4 ± 0.2 spikes/s (Fig. 3E).

Forty-three ventromedial SCN cells were stimulated for 500s and 12 of these showed increased firing rate throughout (baseline 2.9 ± 0.9 spikes/s, stimulation 5.2 ± 1.1 spikes/s; Fig. 4A,B,C). For these 12 cells, the mean change in firing rate was 2.3 ± 0.5 spikes/s (2.9 ± 0.9 spikes/s in the 6 cells in the light phase; 1.7 ±0.4 spikes/s in the 6 cells in the dark phase). The mean change in firing rate for the 31 non-responsive cells was -0.8 ± 0.4 spikes/s (Fig. 4C).

Another two cells responded to optogenetic stimulation with a single burst of increased firing rate in the first 100s of stimulation. These two cells were stimulated for 500s and showed a change in firing rate of 11.8 and 2.4 spikes/s respectively during the first 100s of stimulation only. For these cells, the baseline firing rate was 3.3 ± 0.2 and 7.1 ± 0.3 spikes/s, and the firing rate during the first 100s of stimulation was 15.1 ± 1.1 and 9.5 ± 1.0 spikes/s, respectively.

Twelve ventromedial SCN cells from five non-virus transfected control VP-eGFP rats were also recorded at the beginning of the light phase and the slices exposed to 500s of pulses of blue light. The mean change in firing rate for these control cells was -0.9 ± 0.4 spikes/s (Fig. 4C).

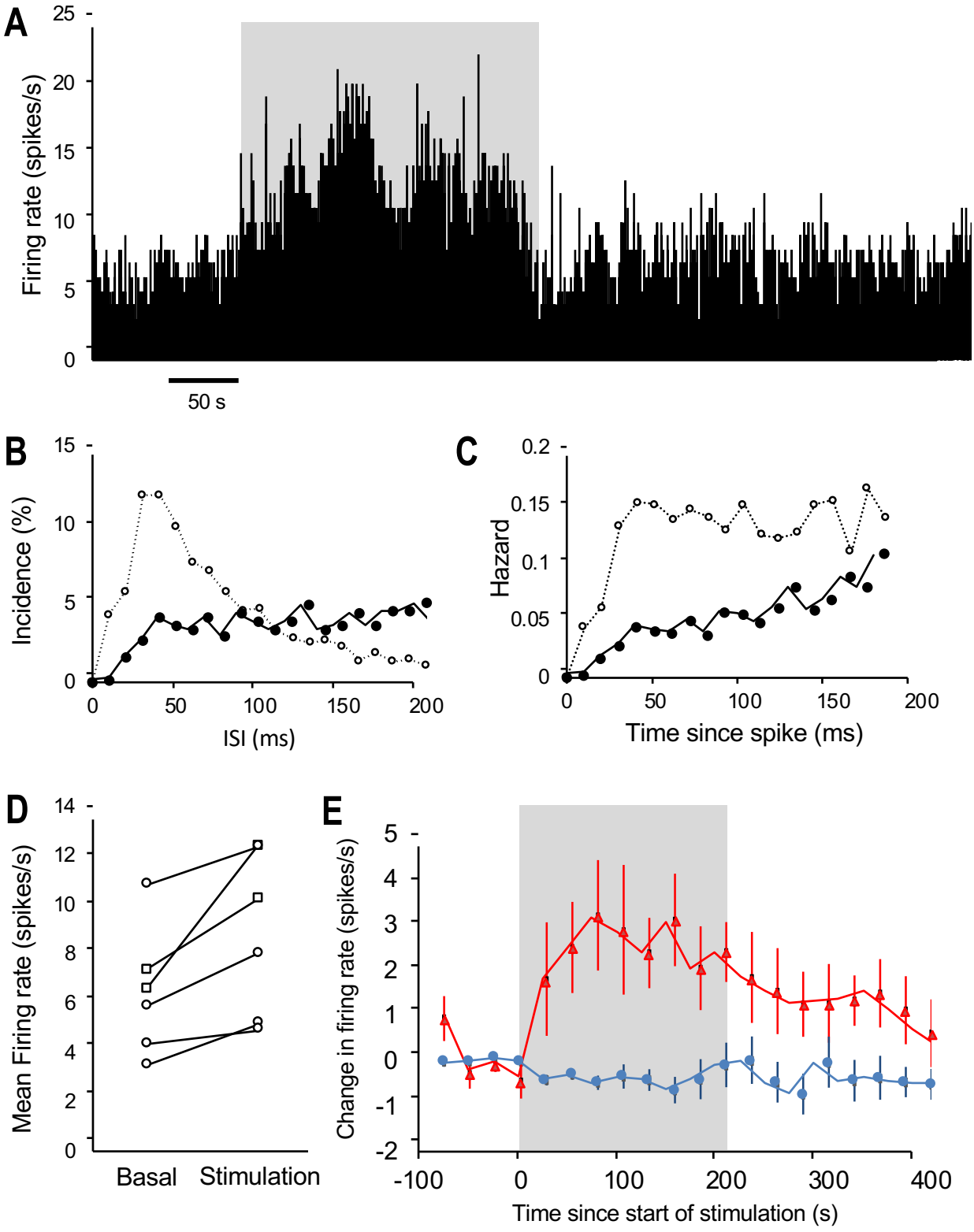

Figure 3. Responses of SCN cells to 200s optogenetic stimulation.
A) Example of an SCN cell showing excitation during 200s of optogenetic stimulation (grey background). **B)** ISI distributions for the 100-s before stimulation (closed circles) and during the 200 s of stimulation (open circles). The functions are normalised to the total number of spikes, so the Incidence plotted is the % of spikes in each 10-ms bin. **C)** Hazard functions corresponding to the ISI distributions in B. **D)** Change in firing rate over time (spikes/s, in 25 s bins; mean ± SEM) for 6 responding cells. Circles = recordings from ZT2, squares = ZT22 (*p=0.016). **E)** Mean (±S.E.) change in firing rate for the 6 responsive cells (red) and 15 non-responding cells (blue) during 200 s of optogenetic stimulation and over the subsequent 200s.

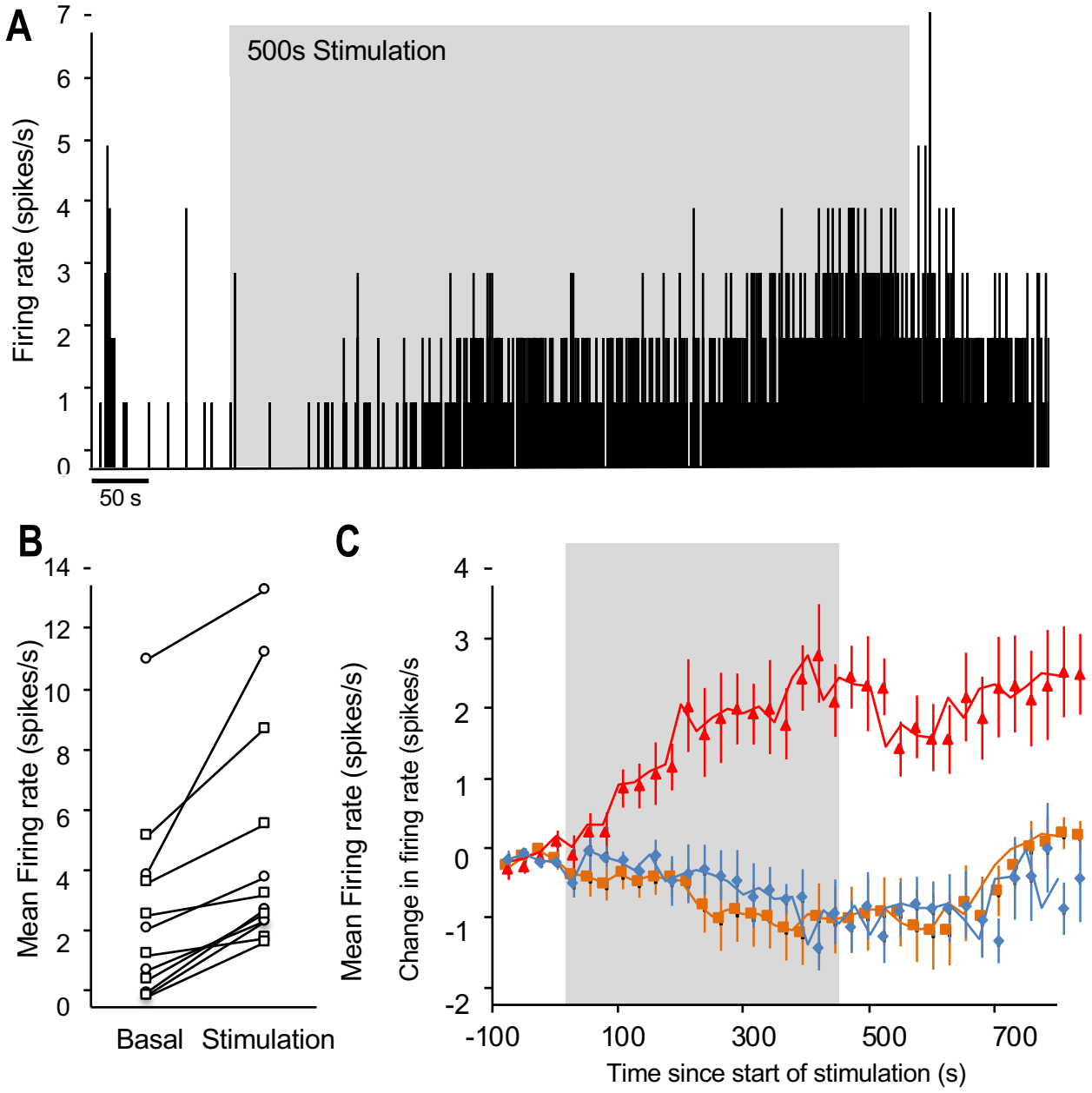

Figure 4) Responses of SCN cells to 500s optogenetic stimulation.
A) Example of SCN cell activated throughout 500s of optogenetic stimulation (grey background). **B)** Firing rate before stimulation and during the last 100s of stimulation for 12 responding cells. Circles = recordings from ZT2, squares = ZT22. (*p=0.0003). **C)** Mean ± SE change in firing rate during optogenetic stimulation for 500s (grey background) for 12 responding cells (red), 32 non-responding cells (orange) and 12 SCN cells from non-virus transfected control rats (blue).

Effects of a vasopressin V1A receptor antagonist

During optogenetic stimulation, a vasopressin V1A receptor antagonist was applied to 27 ventromedial SCN cells. Before application of the antagonist, seven of these cells had responded to optogenetic stimulation with a mean increase in firing rate of 3.7 ± 1.0 spikes/s from a basal rate of 7.4 ± 2.1 spikes/s (Fig. 5A-C). During antagonist application, there was a reduction in firing rate in each of the seven cells (stimulation 11.6 ± 2.2 spikes/s, stimulation/antagonist 9.2 ± 2.3 spikes/s; Fig. 5A-C). By contrast, for the 20 non-responsive SCN cells, application of the antagonist had no significant effect on firing rate (baseline 5.6 ± 0.7 spikes/s, stimulation 5.5 ± 0.6 spikes/s, stimulation with antagonist 5.6 ± 1.1 spikes/s; Fig. 5C). Thus, during optogenetic stimulation, the antagonist reduced the firing rate of the 7 responsive cells by 2.3 ± 0.4 spikes/s, whereas in the 20 cells non-responsive to optogenetic stimulation it produced a mean increase of 0.1 ± 0.7 spikes/s (significant difference between groups, t-test, P=0.003).

Responses of vasopressin expressing SCN cells to optogenetic stimulation

Eight eGFP+ dorsolateral SCN cells from six virus-transfected rats were recorded (Fig. 6A; light phase n=7, dark phase n=1). The spontaneous firing rate of these cells ranged from 0.03 to 14.7 spikes/s with a mean of 4.5 ± 2.0 spikes/s. Optogenetic stimulation had no excitatory effect on any of these eGFP+ cells, and no significant effect overall on the population (baseline 4.5 ± 2.0 spikes/s, stimulation 3.1 ± 1.3 spikes/s; P = 0.11; Fig. 6B,C).

Discussion

Optogenetic activation of VP-RGC axons terminating in the SCN increased the electrical activity of approximately 30% of neurons in the ventromedial SCN. This appeared to be mediated in part by vasopressin as shown by the dampening of stimulation-induced responses with the administration of a vasopressin V1A receptor antagonist, consistent with the hypothesis that vasopressin is released in an activity-dependent manner from the axons of VP-RGCs. No significant effects of the antagonist were seen in any cell that did not respond to optogenetic stimulation.

The most common response to optogenetic stimulation of VP-RGC axons was an increase in firing rate that developed progressively during stimulation and which outlasted the stimulation. Such slowly developing and persistent effects are expected of activity-dependent peptide release (25). RGCs also use glutamate as a neurotransmitter (26). However, the expected response to evoked glutamate release is a rapid onset, adapting

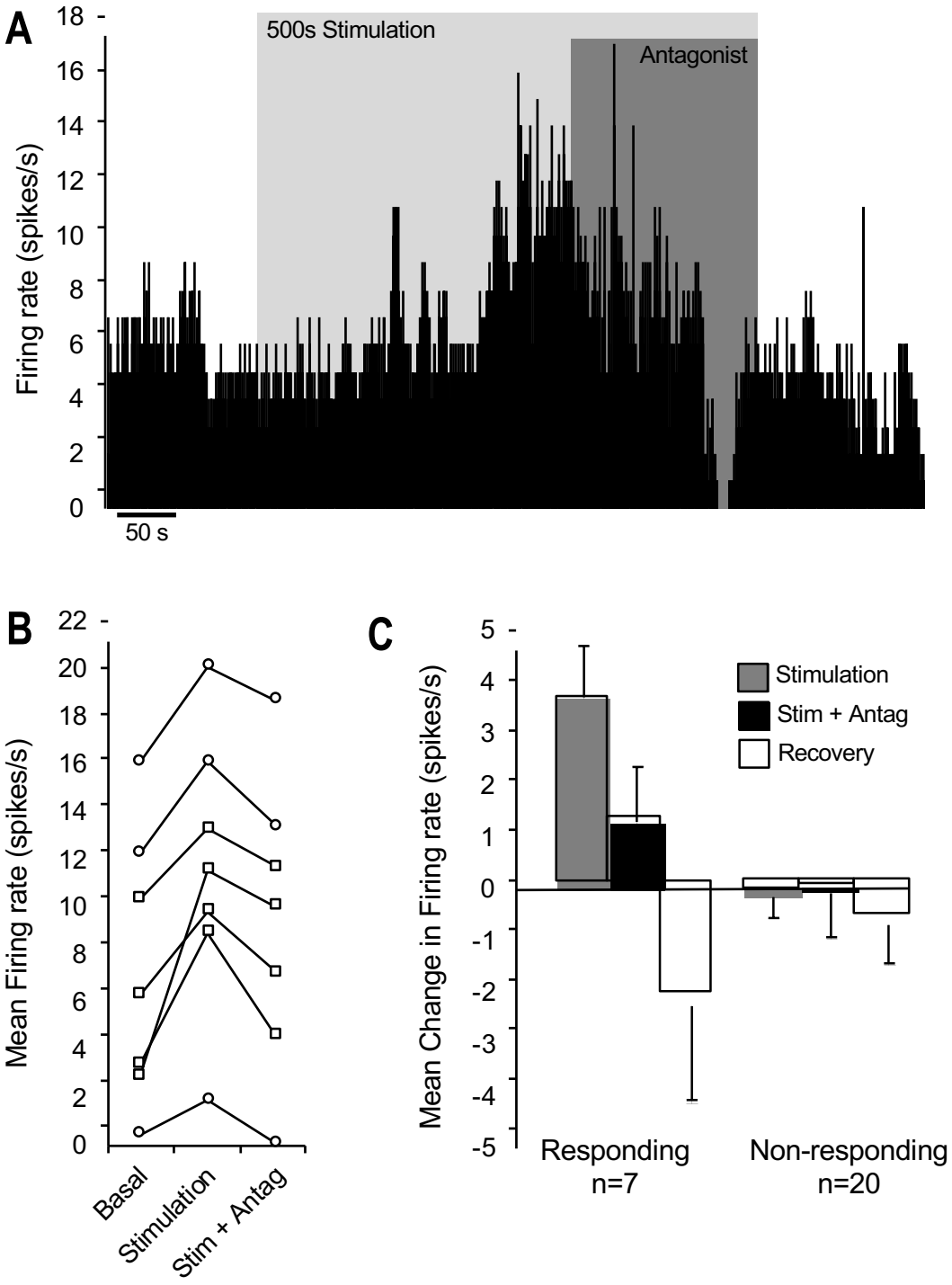

Figure 5) A vasopressin V1A antagonist reduces response to optogenetic stimulation. **A)** Example of SCN cell responding to optogenetic stimulation (light grey background) and application of a vasopressin V1A antagonist (dark grey background). **B)** Mean firing rate (spikes/s; 100s) for baseline, optogenetic stimulation and stimulation in the presence of the antagonist for 7 cells responding to optogenetic stimulation. Circles = recordings from ZT2, squares = ZT22 (Friedman test ($p=0.0003$) followed by Dunn's multiple comparisons (*$p<0.05$)). **C)** Mean ± SE change in firing rate (spikes/s; 100s) during stimulation, stimulation in the presence of the antagonist and recovery for 7 stimulation responding cells and 20 stimulation non-responding cells.

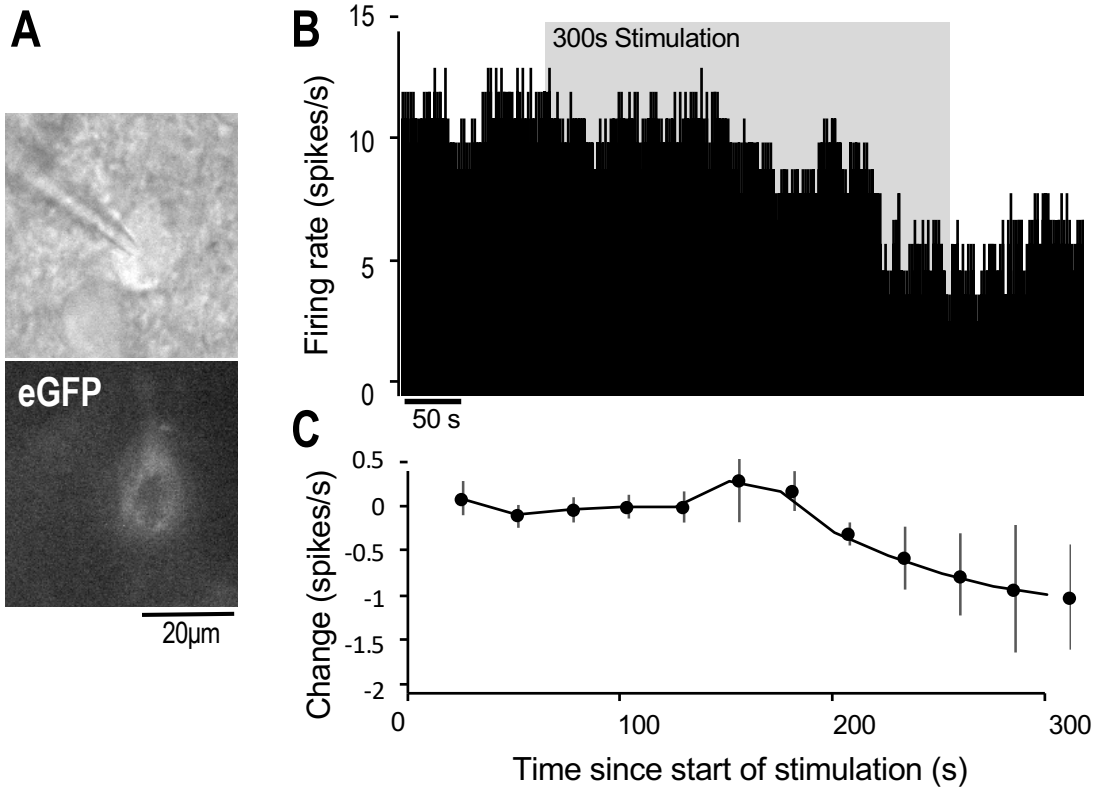

Figure 6) SCN vasopressin cells did not respond to optogenetic stimulation
A) Representative image of SCN dorsolateral eGFP+ cell recorded. **B)** Example of SCN recording from eGFP positive cell with optogenetic stimulation (grey background). **C)** Mean ± SEM change in firing rate during 300s of stimulation (n=8).

response during stimulation, locked to the stimulation pattern with prompt termination at the end of stimulation, very different in all respects from most of the observed responses, although two cells responded with a transient burst of increased firing. It thus appears that, generally, the responses to stimulation reported in these experiments were not mediated monosynaptically by glutamate release. These responses were however blocked by the administration of a vasopressin V1A receptor antagonist.

SCN cells are heterogeneous in their electrophysiological characteristics. Many SCN cells are spontaneously active *in vitro;* in many of these, each spike is followed by an after-hyperpolarisation followed by a progressive repolarisation that reaches spike threshold. This mechanism gives rise to regular spiking at a frequency determined in part by the magnitude and duration of the afterhyperpolarisation. In most other SCN cells, there is again a repolarisation following an afterhyperpolarisation, but the repolarisation does not exceed spike threshold and so spike timing in these cells is more irregular, presumably dominated by the random arrival of synaptic input. Thus Pennartz *et al.* reported that most SCN cells could be classified as Cluster I and II cells that fired spontaneously in a regular and irregular mode respectively (24). The afterhyperpolarisation in cluster I cells is supported by at least three subtypes of K(Ca) channels, including apamin-sensitive channels and iberiotoxin-sensitive channels; these channels are subject to diurnal modulation by the circadian clock leading to the expression of a circadian rhythm in spiking frequency (27).

Pennartz *et al.* observed the after-hyperpolarisations directly by patch-clamp recordings: in the present study used cell-attached recordings to avoid any disruption of the intracellular milieu (24). We noted that spike activity in virtually all SCN neurons was relatively regular, with a CV of less than 1 (which would be indicative of purely random firing), and often very much less than 1 (indicative of very regular firing). However, we could not objectively separate two populations based on this alone. The sequence of afterhyperpolarisation and repolarisation in a spontaneously active cell is reflected in the hazard function, and again we noted that whereas some cells showed an early onset of repolarisation, in many others it was markedly delayed, consistent with a prolonged afterhyperpolarisation. However, we could not objectively separate two populations based on this, nor did we find any evidence that responsiveness to optogenetic stimulation was associated with any observed difference in cell properties.

There is considerable evidence for circadian regulation of potassium currents in the SCN (28, 29), so, in the present study, we recorded SCN cells at the end of the dark phase and at the beginning of the light phase. We observed no significant differences in the mean

spontaneous firing, rate but cells in the light phase showed a wider range of spontaneous firing rates, and also fired less regularly. This is partly consistent with a change in their intrinsic activity-dependent properties; a reduction in the magnitude of the afterhyperpolarisation would be expected to produce both higher firing rates and increased irregularity of firing, but this would not explain why we also saw more slow firing cells in the light phase.

We did not biochemically identify the cells recorded in the ventromedial SCN, but the recording sites are consistent with the distribution VIP and GRP cells in the rat SCN (30). VIP and GRP neurons are part of a complex network within the SCN signalling to other cell types in the dorsolateral SCN to generate rhythms of neuronal activity (31, 32), which are crucial to the functioning and output of the SCN (2). We have previously shown that VP-RGC axons terminate in this region and make close synaptic contacts with both VIP- and GRP-expressing neurons (5).

The shell region of the SCN contains many vasopressin neurons that might also be a source of vasopressin release following optogenetic stimulation. These neurons are primarily situated in the dorsolateral SCN (30) and we have previously shown that VP-RGC axons do not make direct contacts with these vasopressin cells (5). The small population of dorsolateral SCN vasopressin cells (eGFP+) that we recorded from did not respond to optogenetic stimulation. Magnocellular vasopressin neurons are also known to secrete vasopressin from their dendrites in an activity-independent manner (33). Therefore, even in the absence of increased electrical activity, it is possible that these neurons secrete vasopressin into the SCN.

In conclusion, the present study provides evidence for communication between VP-RGCs and ventromedial SCN neurons, supporting the idea that VP-RGCs play an important role in the regulation of the SCN. Various studies have shown that vasopressin is involved in the maintenance and prevention of the maladaptive shifting of circadian rhythms (6, 8, 9). As the disruption of circadian rhythms in humans is associated with a whole variety of diseases and conditions including obesity, cardiovascular disease, depression and cognitive impairment (3, 34-36), there is great interest in understanding the mechanisms underlying circadian dysfunction to identify potential therapeutic targets.

Acknowledgements

Thanks to Dr Fabrice Plaisier and Christiaan Huffles for their help with *in vitro* electrophysiological recordings and Prof Maurice Manning (University of Toledo) for providing

the vasopressin V1A receptor antagonist ((d(CH_2)$_5$^{1}Tyr(Me)^{2}Arg^8)-vasopressin). Supported by a MRC grant awarded to ML and GL (MR/M022838) and the Schaller Research Foundation to VG.

Data sharing: The data that support the findings of this study will be openly available at http://datashare.is.ed.ac.uk/.

References

1. Hastings M, O'Neill JS, Maywood ES. Circadian clocks: regulators of endocrine and metabolic rhythms. *J Endocrinol*. 2007; **195**: 187-98.
2. Colwell CS. Linking neural activity and molecular oscillations in the SCN. *Nat Rev Neurosci*. 2011; **12**: 553-69.
3. LeGates TA, Fernandez DC, Hattar S. Light as a central modulator of circadian rhythms, sleep and affect. *Nat Rev Neurosci*. 2014; **15**: 443-54.
4. Sollars PJ, Pickard GE. The Neurobiology of Circadian Rhythms. *Psychiatr Clin North Am*. 2015; **38**: 645-65.
5. Tsuji T, Allchorne AJ, Zhang M, Tsuji C, Tobin VA, Pineda R, Raftogianni A, Stern JE, Grinevich V, Leng G, Ludwig M. Vasopressin casts light on the suprachiasmatic nucleus. *J Physiol*. 2017; **595**: 3497-514.
6. Kalsbeek A, Fliers E, Hofman MA, Swaab DF, Buijs RM. Vasopressin and the output of the hypothalamic biological clock. *J Neuroendocrinol*. 2010; **22**: 362-72.
7. Watanabe K, Koibuchi N, Ohtake H, Yamaoka S. Circadian rhythms of vasopressin release in primary cultures of rat suprachiasmatic nucleus. *Brain Res*. 1993; **624**: 115-20.
8. Li JD, Burton KJ, Zhang C, Hu SB, Zhou QY. Vasopressin receptor V1a regulates circadian rhythms of locomotor activity and expression of clock-controlled genes in the suprachiasmatic nuclei. *Am J Physiol Regul Integr Comp Physiol*. 2009; **296**: R824-30.
9. Yamaguchi Y, Suzuki T, Mizoro Y, Kori H, Okada K, Chen Y, Fustin JM, Yamazaki F, Mizuguchi N, Zhang J, Dong X, Tsujimoto G, Okuno Y, Doi M, Okamura H. Mice genetically deficient in vasopressin V1a and V1b receptors are resistant to jet lag. *Science*. 2013; **342**: 85-90.
10. Antle MC, Smith VM, Sterniczuk R, Yamakawa GR, Rakai BD. Physiological responses of the circadian clock to acute light exposure at night. *Rev Endocr Metab Disord*. 2009; **10**: 279-91.
11. Ueta Y, Fujihara H, Serino R, Dayanithi G, Ozawa H, Matsuda K, Kawata M, Yamada J, Ueno S, Fukuda A, Murphy D. Transgenic expression of enhanced green fluorescent protein enables direct visualization for physiological studies of vasopressin neurons and isolated nerve terminals of the rat. *Endocrinology*. 2005; **146**: 406-13.
12. Eliava M, et al. A New Population of Parvocellular Oxytocin Neurons Controlling Magnocellular Neuron Activity and Inflammatory Pain Processing. *Neuron*. 2016; **89**: 1291-304.
13. Schatz KC, Brown LM, Barrett AR, Roth LC, Grinevich V, Paul MJ. Viral rescue of magnocellular vasopressin cells in adolescent Brattleboro rats ameliorates diabetes insipidus, but not the hypoaroused phenotype. *Sci Rep-Uk*. 2019; **9**.

14. Boyden ES, Zhang F, Bamberg E, Nagel G, Deisseroth K. Millisecond-timescale, genetically targeted optical control of neural activity. *Nat Neurosci*. 2005; **8**: 1263-8.
15. Hasan MT, et al. A Fear Memory Engram and Its Plasticity in the Hypothalamic Oxytocin System. *Neuron*. 2019; **103**: 133-46.e8.
16. Knobloch HS, Charlet A, Hoffmann LC, Eliava M, Khrulev S, Cetin AH, Osten P, Schwarz MK, Seeburg PH, Stoop R, Grinevich V. Evoked axonal oxytocin release in the central amygdala attenuates fear response. *Neuron*. 2012; **73**: 553-66.
17. Ting JT, Daigle TL, Chen Q, Feng G. Acute brain slice methods for adult and aging animals: application of targeted patch clamp analysis and optogenetics. *Methods Mol Biol*. 2014; **1183:** 221-42.
18. Arrigoni E, Saper CB. What optogenetic stimulation is telling us (and failing to tell us) about fast neurotransmitters and neuromodulators in brain circuits for wake-sleep regulation. *Curr Opin Neurobiol*. 2014; **29:** 165-71.
19. Kruszynski M, Lammek B, Manning M, Seto J, Haldar J, Sawyer WH. [1-beta-Mercapto-beta,beta-cyclopentamethylenepropionic acid),2-(O-methyl)tyrosine]argine-vasopressin and [1-beta-mercapto-beta,beta-cyclopentamethylenepropionic acid)]argine-vasopressine, two highly potent antagonists of the vasopressor response to arginine-vasopressin. *J Med Chem*. 1980; **23**: 364-8.
20. Manning M, Misicka A, Olma A, Bankowski K, Stoev S, Chini B, Durroux T, Mouillac B, Corbani M, Guillon G. Oxytocin and vasopressin agonists and antagonists as research tools and potential therapeutics. *J Neuroendocrinol*. 2012; **24**: 609-28.
21. Schmidt TM, Kofuji P. An isolated retinal preparation to record light response from genetically labeled retinal ganglion cells. *J Vis Exp*. 2011(47).
22. Tsuji T, Tsuji C, Ludwig M, Leng G. The rat suprachiasmatic nucleus: the master clock ticks at 30 Hz. *J Physiol*. 2016; **594**: 3629-50.
23. Sabatier N, Brown CH, Ludwig M, Leng G. Phasic spike patterning in rat supraoptic neurones in vivo and in vitro. *J Physiol*. 2004; **558**: 161-80.
24. Pennartz CM, De Jeu MT, Geurtsen AM, Sluiter AA, Hermes ML. Electrophysiological and morphological heterogeneity of neurons in slices of rat suprachiasmatic nucleus. *J Physiol*. 1998; **506:** 775-93.
25. Bichet DG. Central vasopressin: dendritic and axonal secretion and renal actions. *Clin Kidney J*. 2014; **7**: 242-7.
26. Marc RE, Jones BW. Molecular phenotyping of retinal ganglion cells. *J Neurosci*. 2002; **22**: 413-27.
27. Cloues RK, Sather WA. Afterhyperpolarization regulates firing rate in neurons of the suprachiasmatic nucleus. *J Neurosci*. 2003; **23**: 1593-604.
28. Itri JN, Vosko AM, Schroeder A, Dragich JM, Michel S, Colwell CS. Circadian regulation of a-type potassium currents in the suprachiasmatic nucleus. *J Neurophysiol*. 2010; **103**: 632-40.
29. Farajnia S, Meijer JH, Michel S. Photoperiod Modulates Fast Delayed Rectifier Potassium Currents in the Mammalian Circadian Clock. *ASN Neuro*. 2016; **8**(5).
30. Moore RY, Speh JC, Leak RK. Suprachiasmatic nucleus organization. *Cell Tissue Res*. 2002; **309**: 89-98.
31. Aton SJ, Colwell CS, Harmar AJ, Waschek J, Herzog ED. Vasoactive intestinal polypeptide mediates circadian rhythmicity and synchrony in mammalian clock neurons. *Nat Neurosci*. 2005; **8**: 476-83.
32. Gamble KL, Allen GC, Zhou T, McMahon DG. Gastrin-releasing peptide mediates light-like resetting of the suprachiasmatic nucleus circadian pacemaker through cAMP response element-binding protein and Per1 activation. *J Neurosci*. 2007; **27**: 12078-87.

33. Ludwig M, Bull PM, Tobin VA, Sabatier N, Landgraf R, Dayanithi G, Leng G. Regulation of activity-dependent dendritic vasopressin release from rat supraoptic neurones. *J Physiol*. 2005; **564**: 515-22.
34. Froy O. The circadian clock and metabolism. *Clin Sci (Lond)*. 2011; **120**: 65-72.
35. Hastings MH, Reddy AB, Maywood ES. A clockwork web: circadian timing in brain and periphery, in health and disease. *Nat Rev Neurosci*. 2003; **4**: 649-61.
36. Albrecht U. Timing to perfection: the biology of central and peripheral circadian clocks. *Neuron*. 2012; **74**: 246-60.